Antiangiogenic and Antineuroinflammatory Effects of Kallistatin Through Interactions With the Canonical Wnt Pathway

Xiaochen Liu,[1,2] Bin Zhang,[3] Jeffrey D. McBride,[4] Kevin Zhou,[2] Kyungwon Lee,[4] Yueping Zhou,[1] Zuguo Liu,[1] and Jian-xing Ma[2]

Kallistatin is a member of the serine proteinase inhibitor superfamily. Kallistatin levels have been shown to be decreased in the vitreous while increased in the circulation of patients with diabetic retinopathy (DR). Overactivation of the Wnt pathway is known to play pathogenic roles in DR. To investigate the role of kallistatin in DR and in Wnt pathway activation, we generated kallistatin transgenic (kallistatin-TG) mice overexpressing kallistatin in multiple tissues including the retina. In the oxygen-induced retinopathy (OIR) model, kallistatin overexpression attenuated ischemia-induced retinal neovascularization. In diabetic kallistatin-TG mice, kallistatin overexpression ameliorated retinal vascular leakage, leukostasis, and overexpression of vascular endothelial growth factor and intracellular adhesion molecule. Furthermore, kallistatin overexpression also suppressed Wnt pathway activation in the retinas of the OIR and diabetic models. In diabetic Wnt reporter (BAT-gal) mice, kallistatin overexpression suppressed retinal Wnt reporter activity. In cultured retinal cells, kallistatin blocked Wnt pathway activation induced by high glucose and by Wnt ligand. Coprecipitation and ligand-binding assays both showed that kallistatin binds to a Wnt coreceptor LRP6 with high affinity (K_d = 4.5 nmol/L). These observations suggest that kallistatin is an endogenous antagonist of LRP6 and inhibitor of Wnt signaling. The blockade of Wnt signaling may represent a mechanism for its antiangiogenic and antineuroinflammatory effects. *Diabetes* 62:4228–4238, 2013

A number of natural antiangiogenic factors or angiogenic inhibitors have been identified (1). These endogenous angiogenic inhibitors include several proteins in the serine proteinase inhibitor (SERPIN) superfamily, such as pigment epithelium–derived factor (PEDF), α1-antitrypsin (AAT), and kallistatin (SERPINA4) (2–4). Kallistatin was first identified as a secreted, specific inhibitor of tissue kallikrein (5). Later, kallistatin displayed novel functions independent of its interaction with tissue kallikrein, including inhibition of angiogenesis and tumor growth (4). Like other SERPIN members, kallistatin is expressed not only in the liver but also in the heart, kidney, retina, blood vessels, and many other tissues and cell types (6). The broad tissue distribution of kallistatin suggests that it may confer multiple functions such as regulation of cardiovascular function and blood vessel development (7). The retina is a specialized, vascularized tissue and direct extension of the central nervous system. We previously found that the vitreous levels of kallistatin were significantly reduced in patients with diabetic retinopathy (DR), compared with that in nondiabetic control patients (8). This finding suggests that decreased vitreous levels of kallistatin may contribute to a proangiogenic and proneuroinflammatory environment in DR. Interestingly, similar to other SERPINs, such as PEDF and plasminogen activator inhibitor-1 (SERPINE1), serum kallistatin levels are increased in type 1 diabetic patients and correlate with the presence of microvascular complications (9). This paradoxical trend reflects the need to study the local tissue effects of various SERPINs, since circulation levels of a protein do not always parallel vitreous levels in diabetes. Taken together, these findings suggest a potential role of kallistatin in modulation of microvasculature in diabetic tissues.

Recent evidence suggests that the Wnt pathway mediates inflammatory responses and modulates angiogenesis during development and under disease conditions (10,11). The roles of Wnt signaling in some pathological conditions associated with abnormal neovascularization have been reported. Mutations in components of the Wnt signaling pathway are known to cause several hereditary vascular disorders and defective retinal vascular development (12,13). Further, Wnt signaling upregulates expression of a number of angiogenic and inflammatory factors. Our recent study showed that overactivation of Wnt signaling plays pathogenic roles in diabetic microvascular complications (14).

In the current study, we generated transgenic mice that overexpress and secrete human kallistatin in multiple tissues, with high levels in the retina, and investigated the impacts of kallistatin on ischemia-induced retinal neovascularization, diabetes-induced retinal neuroinflammation, and Wnt signaling activation.

RESEARCH DESIGN AND METHODS

Generation and characterization of kallistatin-transgenic mice. The transgenic mice were generated through a contracted service at Transgenic Animal Facility at Stanford University and confirmed by genotyping with PCR using a forward primer (5′-AGG GAA GAT TGT GGA TTT GG-3′) and a reverse primer (5′-ATG AAG ATA CCA GTG ATG CTC-3′) specific for the human kallistatin cDNA. Retinal structure and function were examined by histology and electroretinography (ERG) analysis.

Retinal angiography. Retinal angiography was performed as previously described (15). Briefly, mice were perfused with 20 mg/mL high–molecular weight (2×10^6) fluorescein isothiocyanate (FITC)-dextran (Sigma, St. Louis, MO). The eyes were fixed and the retina flat mounted. The nonperfused area was measured in the retina using ImageJ software.

Quantification of preretinal vascular cells. Preretinal vascular cells were quantified as previously described (16). Retinal sections from mice with oxygen-induced retinopathy (OIR) were stained with hematoxylin-eosin and examined under a light microscope. The preretinal vascular nuclei were counted in 8 discontinuous sections per eye.

Vascular permeability assay. Retinal vascular permeability was measured using Evans blue as tracer as previously described (17). Briefly, Evans blue was injected through the femoral vein (10 mg/kg body wt) under microscopic inspection. After 2 h circulation, the mice were perfused and the retina was dissected. Evans blue dye in the retina was measured and normalized by total protein concentrations.

Leukostasis assay. The assay was performed following a documented protocol (18). Briefly, mice were perfused through the left ventricle to remove circulating leukocytes in blood vessels. The adherent leukocytes in the vasculature were stained by perfusion with FITC-conjugated concanavalin-A (40 μg/mL; Vector Laboratories, Burlingame, CA) and counted in retinal flat mounts.

ELISA, Western blot analysis, and immunoprecipitation. Intracellular adhesion molecule (ICAM)-1, vascular endothelial growth factor (VEGF), and human kallistatin were measured using ELISA kits purchased from R&D Systems (Minneapolis, MN), and an ELISA kit for both mouse and human kallistatin was purchased from Sino Biological (Beijing, China) according to the manufacturer's instructions.

Western blot analysis was performed as described previously (19). For immunoprecipitation assays, purified protein, human serum, supernatants of cell lysates, and conditioned media were mixed. Protein G agarose resin (Roche Applied Science, Indianapolis, IN), Ni-NTA resin (Novagen, Darmstadt, Germany), or the Myc-tag antibody–conjugated resin (Thermo, Rockford, IL) was added to the cell lysates or conditioned medium following the manufacturer's protocol.

Flow cytometry. Animals were perfused with sterile PBS to remove nonadherent cells from the blood vessels. The retinas were immediately harvested and made into single cell suspensions. For blocking of nonspecific binding, anti-mouse CD16/32 was applied according to the manufacturer's instructions. Isotype controls were included for all of the immunolabeling with FITC-anti-mouse CD45 (BioLegend, San Diego, CA), Brilliant-Violet 421-anti-mouse CD11b (BioLegend), PE-anti-Gr-1 (BioLegend), FITC-anti-mouse-CD3 (BioLegend), and PE-anti-mouse-CD19 (BioLegend). Once settings were optimized, samples were run on a Stratedigm flow cytometer (San Jose, CA), and data were analyzed using FlowJo (Ashland, OR), where gates and instrument settings were defined and set according to back-gating analysis and forward and side scatter characteristics. Leukocyte populations were included and gated based on size to exclude dead or clumped cells.

Protein, plasmid, conditioned medium, transfection, and TOPFLASH assay. His-tagged kallistatin (KS-HIS) and LDL receptor–related protein extracellular domain with a His tag (LRP6N-HIS) were expressed using the pTriE×1.1 vector (Novagen, Darmstadt, Germany). LRP6 with a myc tag (LRP6N-Myc) was expressed in the Pcs2+ vector (Novagen), and the TOPFLASH vector was constructed as previously described (20). The TOPFLASH and *Renilla luciferase* pRL-TK vectors were transfected into the cells, and TOPFLASH activity was measured using the dual luciferase assay (Promega, Madison, WI) and normalized by *R. luciferase* activity.

Statistical analysis. Student *t* test was used for comparison between two groups. ANOVA was used to compare three or more groups. Statistical significance was accepted when the *P* value was <0.05.

RESULTS

Generation of transgenic mice overexpressing kallistatin.
The kallistatin transgene construct contained the full-length human kallistatin cDNA under the control of the chicken β-actin promoter (Supplementary Fig. 1*A*). All of the kallistatin transgenic (kallistatin-TG) mice used in this study were confirmed by genotyping. The kallistatin transgene expression was confirmed by ELISA using the serum from kallistatin-TG mice (Supplementary Fig. 1*B*). As shown by ELISA, the kallistatin transgene was highly expressed in the retina of 4-month-old kallistatin-TG mice (Supplementary Fig. 1*C*). We measured endogenous retinal mouse kallistatin using ELISA that detects both mouse and human kallistatins to clarify that the levels of total kallistatin levels in the transgenic mice are within reasonable range above endogenous mouse kallistatin (approximately fourfold) (Supplementary Fig. 1*D*).

For determination of whether kallistatin overexpression in the retina affects retinal development, ocular sections from WT and kallistatin-TG mice were examined by microscopy. At 4 months of age, there were no detectable differences in the histological structure or the nuclear layers of the retinas between WT and kallistatin-TG mice (Supplementary Fig. 2*A*).

As measured by optical coherence tomography, the average retinal thickness in kallistatin-TG mice was not significantly different from that in age-matched WT mice (Supplementary Fig. 2*B*). Furthermore, there were no significant differences in the dark-adapted (scotopic or rod associated) or light-adapted (photopic or cone associated) ERG responses between WT and kallistatin-TG mice (Supplementary Fig. 2*C*). Overall, these results suggest that kallistatin-TG mice do not manifest structural or functional defects in the retina under normal conditions.

Kallistatin overexpression inhibits retinal neovascularization in the OIR model.
The impact of kallistatin overexpression on ischemia-induced retinopathy was evaluated using the OIR model (16). After kallistatin-TG and WT mice were exposed to 75% oxygen from postnatal day 7 (P7) to P12, the retinal vasculature was examined at P18. Comparison of retinal vasculature showed that the retinas in kallistatin-TG mice with OIR developed less severe retinal neovascularization compared with WT mice with OIR (Fig. 1*A*). As enlarged nonperfused area is known to correlate with severity of retinopathy in the OIR model, we also quantified nonperfused area in retinal whole mounts using a computer-based measurement. The results showed that kallistatin-TG mice with OIR had significantly smaller nonperfused areas compared with WT mice with OIR (Fig. 1*B*).

Preretinal neovascularization and retinal proinflammatory cytokines are reduced in kallistatin-TG mice with OIR.
Preretinal neovascularization is a characteristic of ischemia-induced neovascularization in the OIR model and humans with proliferative DR (16,21). The retinal neovascular cells growing into the vitreous space were counted following an established method (16). The results showed that kallistatin-TG mice with OIR developed significantly fewer neovascular cells in the vitreous compared with WT mice with OIR at P18 (Fig. 1*C* and *D*).

Previous studies have shown that retinal neuroinflammation is an important feature of OIR and human DR (22,23). For examination of retinal neuroinflammation, retinal levels of VEGF and ICAM-1 were measured by ELISA. The results showed that retinal levels of VEGF and ICAM-1 were significantly lower in kallistatin-TG mice with OIR compared with in WT mice with OIR at P18 (Fig. 1*E*), suggesting that kallistatin overexpression inhibits retinal neuroinflammation induced by OIR.

Kallistatin overexpression inhibits retinal neuroinflammation and vascular leakage in a genetic model of type 1 diabetes.
To examine the antineuroinflammatory effect of kallistatin in DR, we genetically crossed kallistatin-TG mice with Akita mice, a genetic model of type 1 diabetes, to induce diabetes in kallistatin-TG mice (Akita×kallistatin-TG). Akita×kallistatin-TG mice developed hyperglycemia levels similar to Akita mice without the kallistatin transgene. At 5 months of age, adherent leukocytes in retinal vasculature were visualized using a leukostasis assay, and the result showed that Akita mice had significantly increased leukocytes adhering to the retinal vasculature compared with WT mice (Fig. 2*A* and *B*). As measured by ELISA, retinal levels of ICAM-1, an adhesion
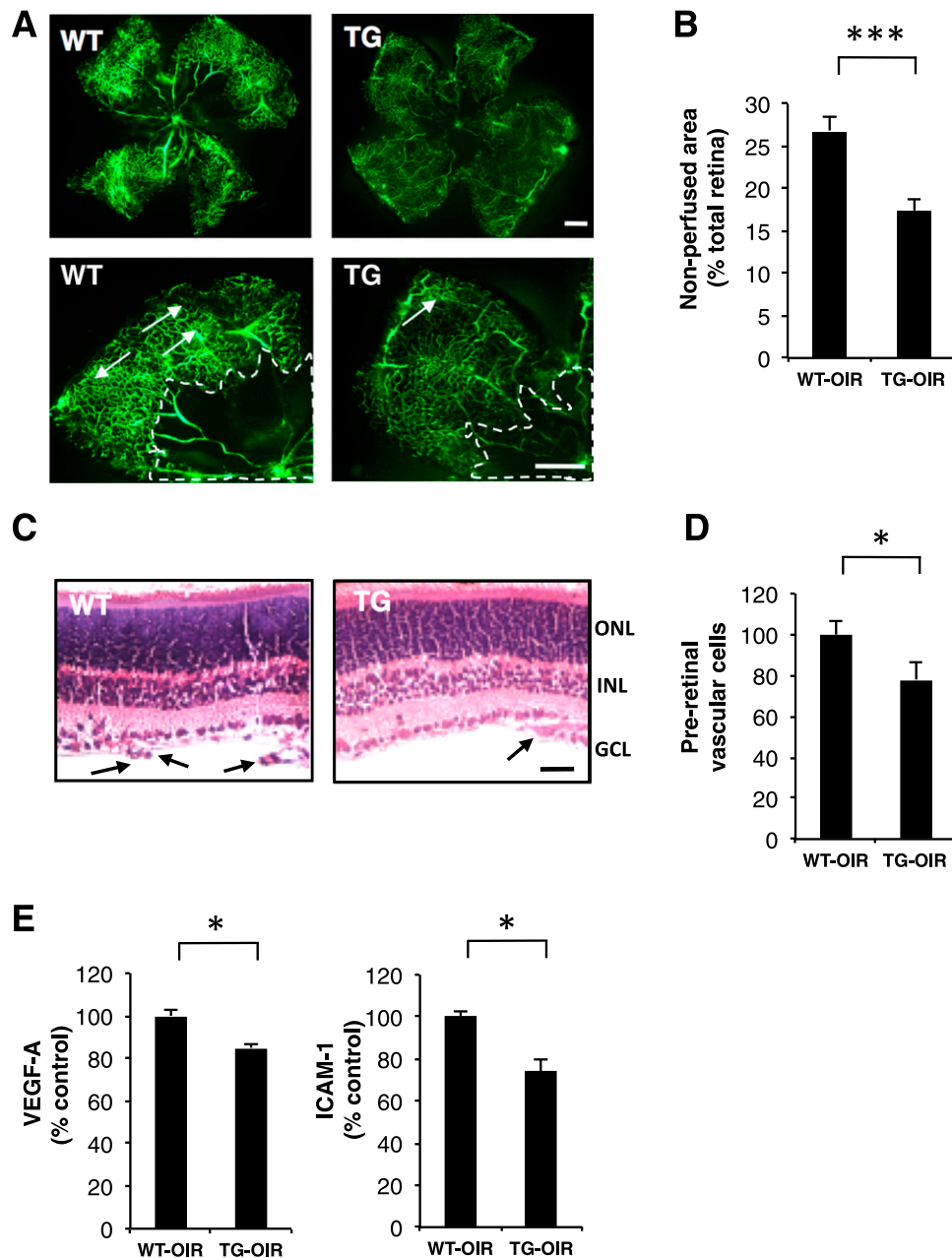
FIG. 1. Alleviated retinal neovascularization and retinal neuroinflammation in the kallistatin-TG mice with OIR. Kallistatin-TG and WT mice were exposed to 75% oxygen from P7 to P12. Angiography was performed using FITC-dextran at P18 and with the retina flat mounted. A: Representative retinal angiographs from the eyes of WT and kallistatin-TG mice with OIR. The white arrows indicate neovascular tufts in the retina. The white dotted line outlines a vascular area in the central retinal. Scale bar: 100 μm. B: Quantification of nonperfused area. Retinal nonperfused area was semiquantified using ImageJ software and expressed as % of the whole area of the retina. $n = 6–9$. At P18, the eyes of kallistatin-TG and WT mice with OIR were fixed, sectioned, and stained with H-E. C: Representative retinal sections from WT and kallistatin-TG mice with OIR. Arrows indicate preretinal vascular cells. Scale bar: 50 μm. D: Preretinal vascular cells were quantified and compared between WT and kallistatin-TG mice with OIR. $n = 8$. E: Retinal levels of VEGF and ICAM-1 were measured with ELISA and expressed as percentages of the respective WT control. $n = 8$. All values are mean ± SD. *$P < 0.05$, ***$P < 0.001$.

molecule responsible for leukostasis, were also significantly elevated in the retina of Akita mice compared with WT mice (Fig. 2C). In contrast, Akita×kallistatin-TG mice showed significantly fewer leukocytes adhering to the retinal vasculature and had significantly lower ICAM-1 levels in the retina compared with in age-matched Akita mice without the transgene (Fig. 2A–C). Purified kallistatin downregulated ICAM-1 expression in a concentration-dependent manner in human retinal capillary endothelial cells (Supplementary Fig. 3). As shown by flow cytometry, the CD11b^{+} leukocytes were significantly elevated in Akita retinas after perfusion, and Akita×kallistatin-TG mice had significantly fewer CD11b^{+} leukocytes in the retina (Supplementary Fig. 4A and B). Gr-1^{+} leukocytes, CD19^{+} B lymphocytes, and CD3^{+} T lymphocytes were not significantly increased in Akita retinas (Supplementary Fig. 4C–H).

As the blood-retinal barrier breakdown in diabetes is a major cause of diabetic retinal edema, we measured retinal vascular leakage using the permeability assay. At 5 months of age, Akita mice showed significantly increased
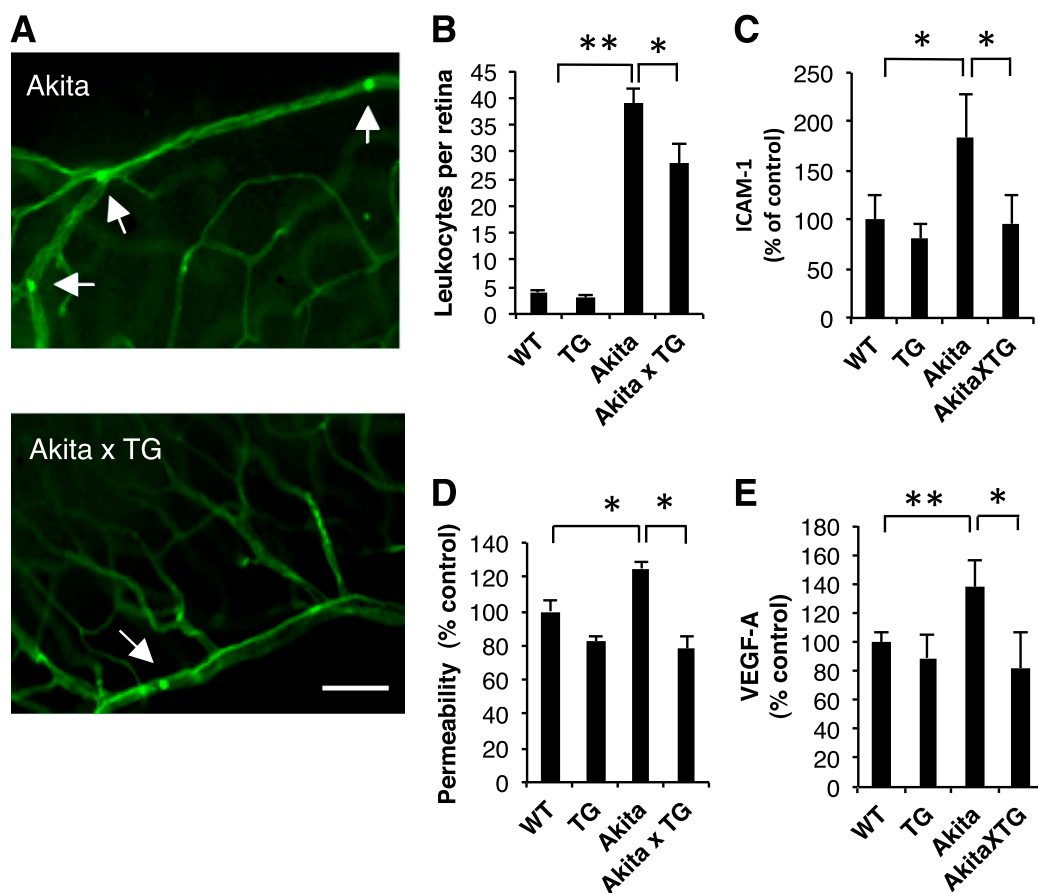
FIG. 2. Decreased retinal neuroinflammation and retinal vascular leakage in diabetic kallistatin-TG mice. Akita mice and Akita×kallistatin-TG mice at 5 months of age were used for leukostasis assay. *A*: Adherent leukocytes (arrow) were stained with FITC-conjugated concanavalin-A in the retinal vasculature. The retinal vasculature and leukocytes were visualized in retinal flat mounts under a fluorescence microscope. Scale bar: 50 μm. *B*: Adherent leukocytes in the retinal vasculature were counted in age-matched WT, kallistatin-TG, Akita, and Akita×kallistatin-TG mice. $n = 7–10$. *C*: Retinal levels of soluble ICAM-1 were measured by ELISA in age-matched WT, kallistatin-TG, Akita, and Akita×kallistatin-TG mice and expressed as percentages of the respective WT control. *D*: Retinal vascular permeability of WT, kallistatin-TG, Akita, and Akita×kallistatin-TG mice was measured using Evans blue as a tracer, normalized by retinal protein concentrations, and expressed as a percentage of the permeability in WT control. *E*: Retinal levels of VEGF-A were measured by ELISA in WT, kallistatin-TG, Akita, and Akita×kallistatin-TG mice and expressed as percentages of the respective WT control. All values are mean ± SD. *$P < 0.05$, **$P < 0.01$.

retinal vascular permeability and increased retinal VEGF levels compared with WT mice (Fig. 2*D* and *E*). Akita×kallistatin-TG mice showed significantly reduced retinal vascular leakage and VEGF levels compared with age-matched Akita mice (Fig. 2*D* and *E*). Taken together, these results support the antineuroinflammatory effect of kallistatin.

Kallistatin inhibits Wnt signaling in the retina of OIR mice and diabetic mice. Our previous studies showed that aberrant activation of the canonical Wnt pathway plays an important pathogenic role in retinal neovascularization and neuroinflammation in both OIR and diabetic animal models (14). To evaluate the effects of kallistatin on the Wnt signaling pathway activation induced by OIR and diabetes, we examined LRP6 and nonphosphorylated β-catenin (non-pi-β-catenin) levels in the retinas with OIR and diabetic mice using Western blot analysis. The results revealed that LRP6 and non-pi-β-catenin levels were significantly lower in the retina of kallistatin-TG mice with OIR compared with in WT mice with OIR, suggesting a suppressed Wnt signaling activity (Fig. 3*A* and *C*).

Furthermore, Western blot analysis showed that LRP6 and non-pi-β-catenin levels in the retinas were increased in the Akita mice at 5 months of age compared with

age-matched WT mice (Fig. 3*B* and *D*), consistent with our previous report that the Wnt signaling pathway is activated in DR (14). In contrast, Akita×kallistatin-TG mice at the same age have significantly lower LRP6 and non-pi-β-catenin levels in the retina compared with Akita mice (Fig. 3*B* and *D*). These findings indicate that kallistatin inhibits retinal Wnt signaling induced by diabetes.

For further confirmation that kallistatin blocks the Wnt pathway in vivo, we measured the transcriptional activity of β-catenin in the retina using reporter mice. We crossed kallistatin-TG mice with BAT-gal reporter mice, which express the β-galactosidase reporter gene under the control of a promoter containing T-cell factor (TCF)/β-catenin–binding sites (BAT-gal×kallistatin-TG). Diabetes was induced in the BAT-gal mice and BAT-gal×kallistatin-TG mice by injections of streptozocin (STZ). Three months after the onset of diabetes, the retinas were stained with X-gal to evaluate the activity of β-galactosidase reporter. Diabetic BAT-gal mice showed more intense X-gal staining in the retina compared with nondiabetic BAT-gal mice, further confirming the diabetes-induced activation of Wnt signaling in the retina. Under the same conditions, diabetic BAT-gal×kallistatin-TG mice showed reduced X-gal staining in the retina compared with age-matched diabetic BAT-gal
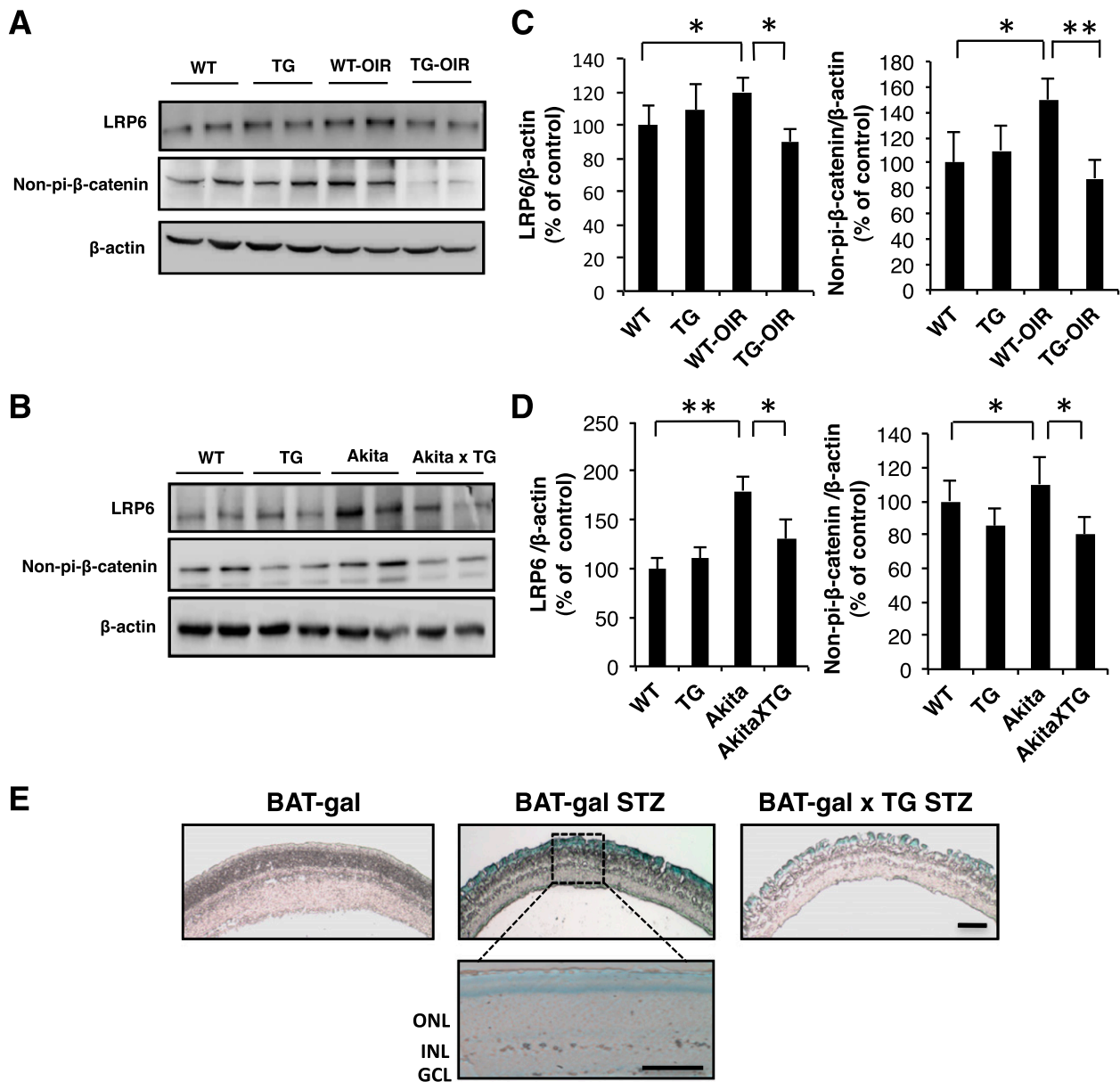
FIG. 3. Kallistatin blocks Wnt signaling in the retina with OIR and diabetic mice. *A*: LRP6 and non-pi-β-catenin in the retinas of WT and kallistatin-TG mice without or with OIR were measured by Western blot analysis. *B*: LRP6 and non-pi-β-catenin in the retinas of WT, kallistatin-TG, Akita, and Akita×kallistatin-TG mice were measured by Western blot analysis. *C* and *D*: The Western blotting results were semiquantified by densitometry, normalized by β-actin levels, averaged in three independent experiments, and expressed as % of the respective WT control. All values are mean ± SD. *n* = 9. *P < 0.05, **P < 0.01. *E*: X-gal staining of retinal sections in BAT-gal mice. Retinas from nondiabetic BAT-gal (as control) mice, STZ diabetic BAT-gal mice, and diabetic BAT-gal×kallistatin-TG mice were harvested at 3 months post–induction of diabetes. The retinas were fixed for 30 min and then incubated at 37°C overnight in X-gal staining solution and sectioned according to the manufacturer's instructions. GCL, ganglion cell layer; INL, inner nuclear layer; ONL, outer nuclear layer. Scale bar: 100 μm.

mice (Fig. 3*E*), confirming that kallistatin overexpression attenuated diabetes-induced activation of Wnt signaling in the retina.

Kallistatin inhibits transcriptional activity of β-catenin induced by Wnt ligand. For determination of whether kallistatin has direct inhibition of Wnt signaling activated by Wnt ligand, hTERT-RPE-1 cells were cotransfected with kallistatin expression vector with the TOPFLASH vector, which expresses a luciferase reporter gene under the control of a promoter containing TCF/β-catenin–binding sites. As shown by luciferase assay, the cells transfected with a plasmid expressing kallistatin inhibited transcriptional activity of β-catenin in a concentration-dependent

manner (Fig. 4*A*). Additionally, the transfected cells were treated with Wnt3a conditioned medium (WCM) after the transfection of the kallistatin expression plasmid and TOPFLASH vector, with L cell–conditioned medium (LCM) as control (Fig. 4*B*). The Wnt3a-induced TOPFLASH activity was also inhibited by kallistatin expression vector in a concentration-dependent manner (Fig. 4*B*).

We also evaluated the inhibitory effect of kallistatin on Wnt signaling induced by transfection of LRP6 expression plasmid (1 μg). The expression plasmids of LRP6 and kallistatin were cotransfected into HEK293T cells, which express low levels of endogenous LRP6. The transfected cells were then treated with WCM for 24 h, with LCM as
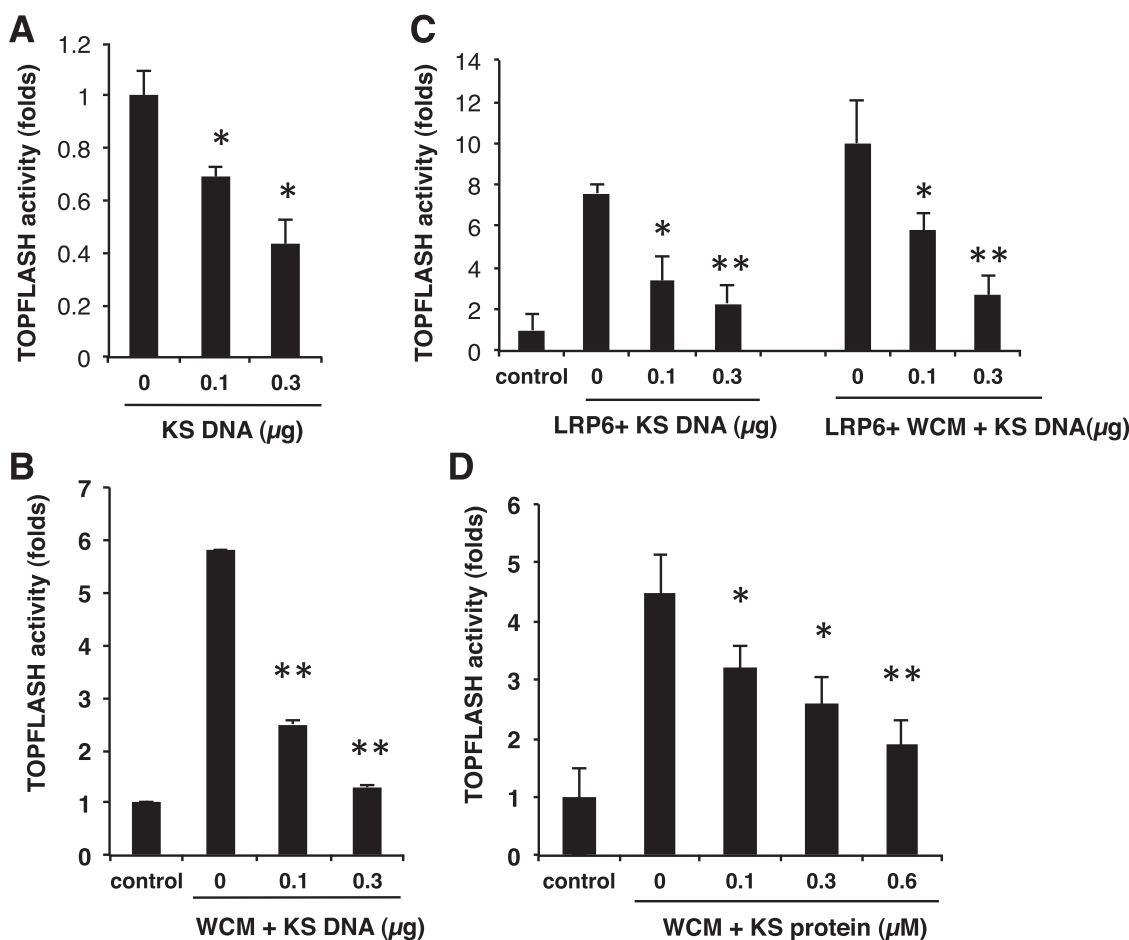
FIG. 4. Kallistatin inhibits TOPFLASH activity induced by Wnt3A and LRP6. *A*: hTERT-RPE-1 cells were transfected with the TOPFLASH vector and 0.1 and 0.3 μg of a kallistatin (KS) expression vector. Total DNA concentration in each well was brought to the same by addition of an empty vector. TOPFLASH activity was measured using luciferase assay. *B*: The cells were transfected with 0.1 and 0.3 μg kallistatin expression vector and then exposed to WCM for 24 h, with the same volume of LCM as control. TOPFLASH activity was measured using luciferase assay. *C*: HEK293T cells were transfected with the TOPFLASH vector and the kallistatin expression plasmid or empty control vectors. TOPFLASH activity was induced by transfection of expression plasmid of LRP6 (1 μg) and by the LRP6 expression plasmid plus WCM. TOPFLASH activity was measured using luciferase assay. *D*: hTERT-RPE-1 cells were transfected with the TOPFLASH vector. The cells were exposed to LCM or WCM for 24 h, incubated with different concentrations of purified kallistatin protein. TOPFLASH activity was measured using luciferase assay. All values are mean ± SD. $n = 6$. *$P < 0.05$, **$P < 0.01$.

control. TOPFLASH activities were significantly increased by transfection of LRP6 and treatment of Wnt3a, which was attenuated by kallistatin expression in a concentration-dependent manner (Fig. 4*C*). Furthermore, hTERT-RPE-1 cells were treated with various concentrations of purified kallistatin protein after transfection with the TOPFLASH vector. The TOPFLASH activity was also inhibited by kallistatin protein in a concentration-dependent manner (Fig. 4*D*). These results indicate that kallistatin inhibits Wnt signaling induced by LRP6 overexpression and by Wnt3a.

In addition to RPE cells, retinal Müller cells and endothelial cells are known to play important roles in DR (24,25). To further confirm that kallistatin inhibits Wnt signaling in Müller cells and endothelial cells, we used lentiviral infection to deliver the TCF/lymphoid enhancer factor–responsive elements (driving luciferase expression) into human Müller cells (HMCs) and human retinal capillary endothelial cells. The cells were then treated to WCM to activate Wnt signaling, with LCM as control. Purified kallistatin was added to the culture medium simultaneously. WCM-induced TOPFLASH activity was inhibited

by kallistatin protein in a concentration-dependent manner (Supplementary Fig. 5).

For determination of whether kallistatin also inhibits Wnt signaling activated intracellularly, LiCl, a glycogen synthase kinase (GSK)-3β inhibitor, was used to activate Wnt signaling at the level of GSK-3β. hTERT-RPE-1 cells were treated with 10 mmol/L LiCl or 10 mmol/L NaCl (as control) after transfection with the TOPFLASH vector and different amounts of the plasmid expressing kallistatin or treated with 0.6 μmol/L purified kallistatin protein. As shown by luciferase assay, LiCl-induced activation of β-catenin was not inhibited by the kallistatin expression vector or by purified kallistatin protein (Supplementary Fig. 6). These findings suggest that kallistatin inhibits the Wnt pathway at the extracellular or the receptor level.

Kallistatin blocks Wnt signaling and downregulates Wnt target genes induced by high glucose and Wnt ligand in cultured retinal cells. For evaluation of the direct effect of kallistatin on Wnt pathway activation induced by Wnt ligand or high glucose, ARPE19 cells were exposed to high-glucose medium (30 mmol/L D-glucose) (HG) or 20% WCM. As shown by Western blot analysis using an antibody

specific for phosphorylated LRP6 (pi-LRP6), phosphorylation of LRP6 was induced by 24-h treatment of HG or WCM compared with that in control cells exposed to L-glucose medium (LG) (5 mmol/L D-glucose and 25 mmol/L L-glucose) or control LCM (Fig. 5A and C). Purified kallistatin (0.6 μmol/L) decreased the pi-LRP6 levels induced by HG and WCM (Fig. 5A–D)

Tumor necrosis factor (TNF)-α and VEGF are known to be regulated by the Wnt signaling pathway and play crucial roles in neuroinflammation and angiogenesis (26). As shown by Western blot analysis in ARPE19 cells,

overexpression of TNF-α and VEGF induced by HG was attenuated by purified kallistatin protein in a concentration-dependent manner (Fig. 5E and F). Taking together, these results suggest that kallistatin directly inhibits Wnt pathway activation and downregulates its target genes, which may represent a major mechanism by which kallistatin inhibits neuroinflammation and angiogenesis.

Kallistatin binds to LRP6 with high affinity. To reveal possible interactions of kallistatin with LRP6 on the cell surface, we incubated human serum, which contains high levels of kallistatin, overnight with conditioned medium
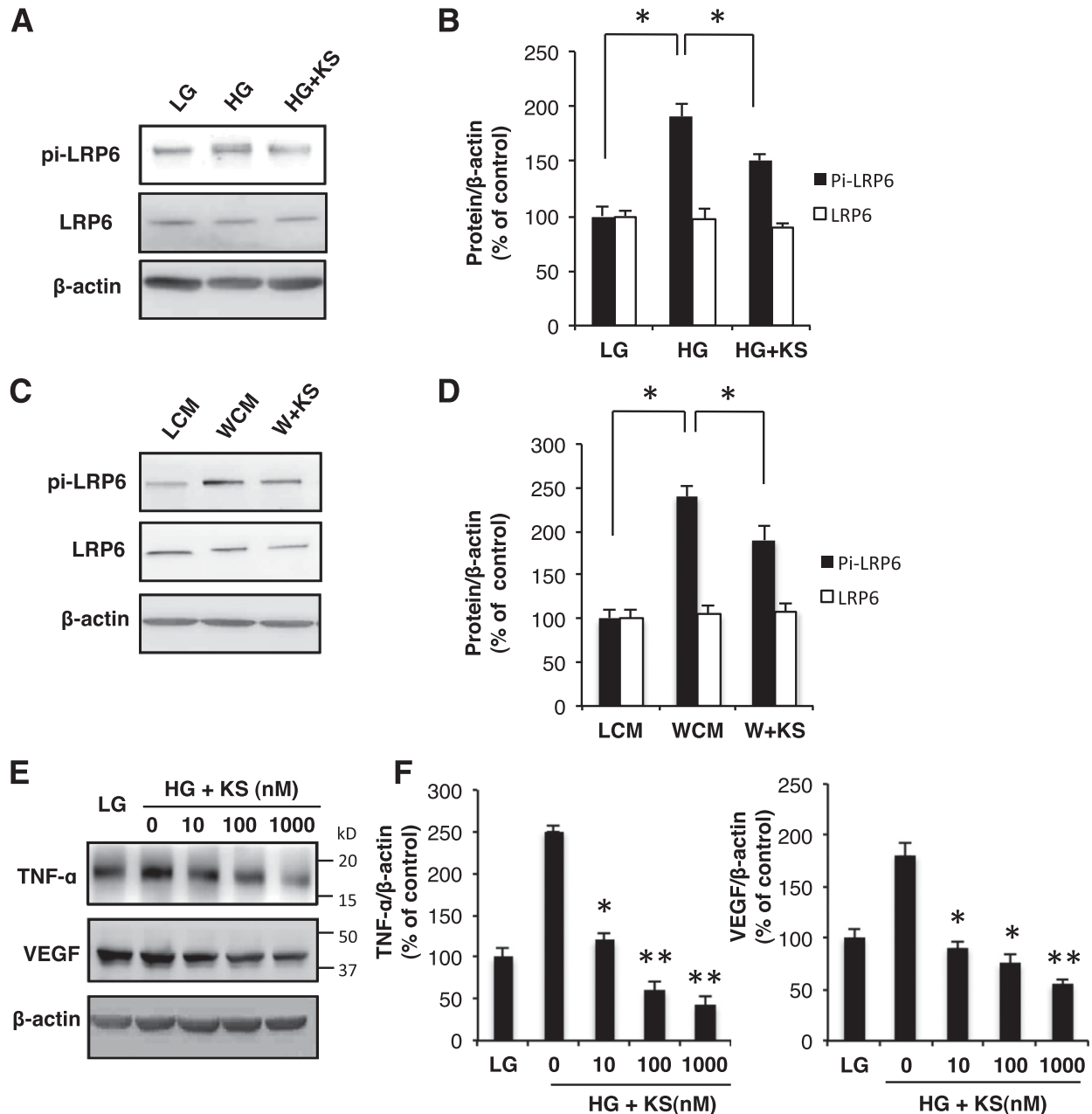
FIG. 5. Kallistatin (KS) inhibits Wnt signaling induced by high glucose and Wnt ligand. A: ARPE19 cells were exposed to HG with 0.6 μmol/L purified kallistatin protein for 24 h, with LG as control. pi-LRP6 and total LRP6 were measured by Western blot analysis. C: The cells were exposed to WCM with 0.6 μmol/L purified kallistatin for 24 h, with LCM as control. pi-LRP6 and total LRP6 were measured using Western blot analysis. E: The cells were exposed to HG with 0, 10, 100, and 1,000 nmol/L purified kallistatin protein for 24 h, with LCM as control. Total protein concentrations in each well were brought to the same level by the addition of BSA. TNF-α and VEGF were measured by Western blot analysis. B, D, and F: The Western blots shown in A, C, and E were semiquantified by densitometry, normalized by β-actin levels, and expressed as % of the LCM or LG control. All values are mean ± SD. n = 6. *P < 0.05, **P < 0.01. W+KS, Wnt-conditioned media + kallistatin.

overexpressing LRP6N-Myc. LRP6N-Myc was then immunoprecipitated with an anti-Myc antibody. As shown by Western blot analysis of the precipitated proteins, kallistatin in the human serum was coprecipitated with LRP6N-Myc (Fig. 6A), indicating that kallistatin binds to LRP6N.

For further confirmation of the interactions between kallistatin and LRP6, purified kallistatin-HIS protein was incubated with conditioned medium containing Myc-tagged extracellular domain of LRP6 (LRP6N-Myc) overnight, and kallistatin-HIS was pulled down using Ni-agarose. The results showed that LRP6N-Myc was coprecipitated with purified kallistatin-HIS (Fig. 6B) (purity of kallistatin-HIS purified protein shown in Supplementary Fig. 7).

For confirmation that the interactions between LRP6 and kallistatin are specific, conditioned media containing either the cysteine-rich domain of the Frizzled 8 receptor (Fz8CRD with a human IgG-tag) or the extracellular domain of LDL receptor (LDLRN-Myc), a receptor in the same family of LRP6, were separately incubated with kallistatin-HIS–conditioned medium. Kallistatin-His was pulled down by Ni-agarose, and the precipitates and input samples were immunoblotted with anti-IgG, anti–Myc tag and anti–HIS tag antibodies. Neither Fz8CRD-IgG nor LDLRN-Myc was coprecipitated with kallistatin-HIS (Fig. 6C and D). To further confirm that the binding of kallistatin and LRP6 was not through the HIS tag, recombinant
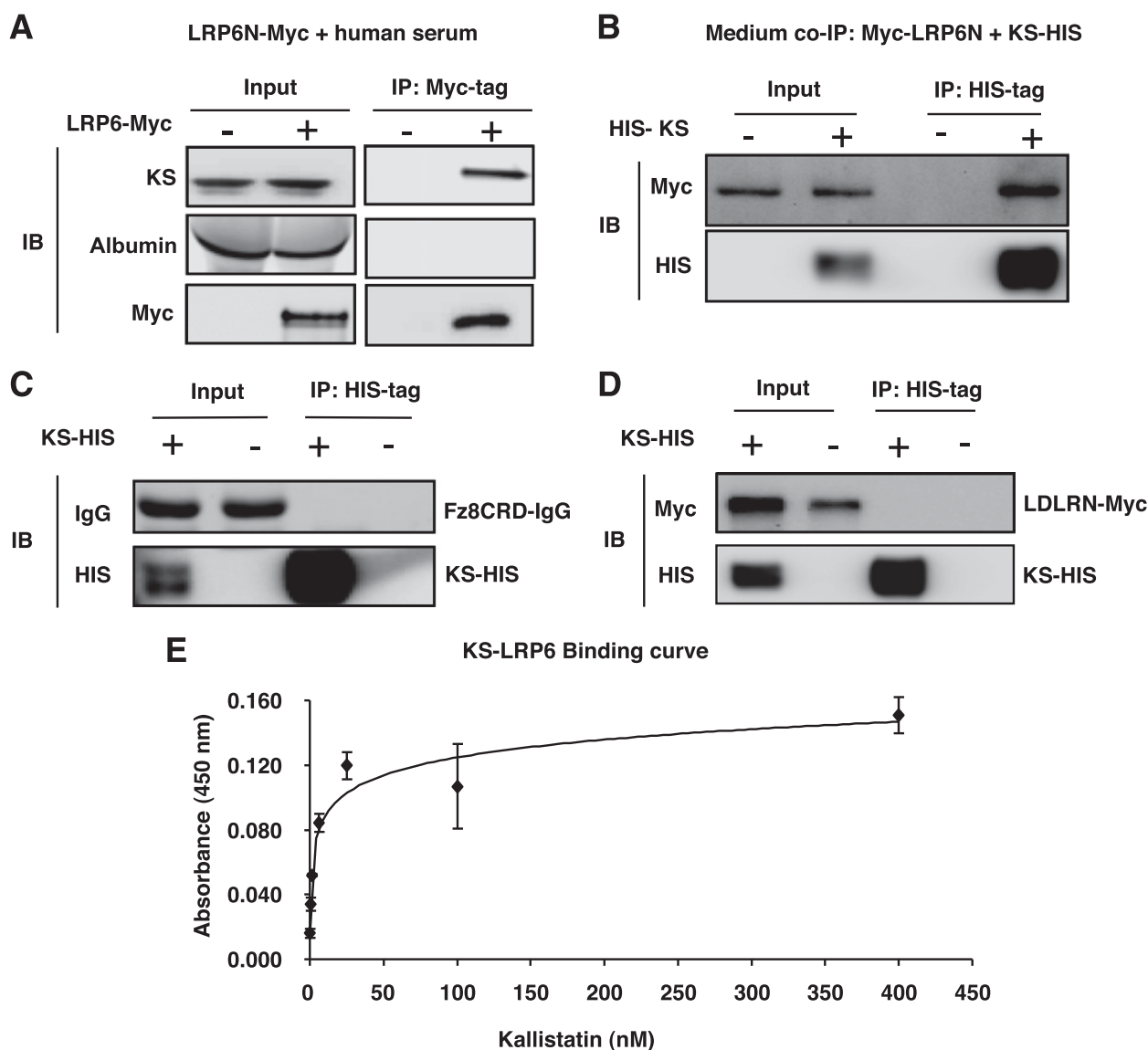
FIG. 6. Kallistatin specifically binds to the extracellular domain of LRP6 with high affinity. A: The human serum was incubated with the conditioned medium expressing LRP6N-Myc followed by immunoprecipitation using the anti–Myc-tag antibody–conjugated resin. Precipitates and input samples were immunoblotted (IB) with anti-kallistatin (KS), -albumin, and –Myc-tag antibodies. B: Immunoprecipitation was performed with the Ni-NTA resin in LRP6N-Myc conditioned medium with or without recombinant KS-HIS. Precipitates and input samples were immunoblotted with anti–Myc-tag and anti–HIS-tag antibodies to detect LRP6N-Myc and KS-HIS protein. C and D: Negative control for coimmunoprecipitation. Immunoprecipitation was performed with the Ni-NTA resin (Novagen, Madison, WI) in Fz8CRD-IgG (CRD domain of Fz-8 with human IgG tag) and LDLRN-Myc–conditioned medium incubated with recombinant KS-HIS. Precipitates and input samples were immunoblotted with antibodies as indicated to identify Fz8CRD-IgG, KS-HIS, and LDLRN-Myc proteins in the precipitates. E: ELISA plates were coated with conditioned medium of LRP6N and LDLRN (negative control) overnight. Different concentrations of purified kallistatin were incubated in the wells. The signals were developed using a Biotin-labeled secondary antibody for kallistatin and measured by absorbance at 450 nm using a microplate reader. The binding value at each concentration was plotted after subtraction of that of nonspecific binding to LDLRN (mean ± SD, $n = 5$).

cellular retinol-binding protein with a HIS tag (CRBP-HIS) was used for coprecipitation assay with LRP6 (Supplementary Fig. 8). CRBP-HIS was not pulled down by LRP6. These observations suggest that kallistatin specifically binds to the extracellular domain of LRP6.

For determination of the binding affinity of kallistatin to LRP6N, conditioned medium of LRP6N-Myc was used to coat the wells of an ELISA plate overnight, and different concentrations of purified kallistatin protein were incubated in the wells followed by thorough washes to remove unbound kallistatin. A biotin-conjugated anti-kallistatin monoclonal antibody was incubated in the wells as the detection antibody. Kallistatin displayed a concentration-dependent and saturable binding to the extracellular domain of LRP6, with a calculated K_d = 4.5 nmol/L (Fig. 6E). These results support that kallistatin inhibits Wnt signaling via specific binding to the extracellular domain of LRP6 with high affinity.

DISCUSSION

Although decreased kallistatin levels in the vitreous from human patients with DR were reported >10 years ago (8), the role of kallistatin in DR was previously unknown. The current study showed that overexpression of kallistatin in the retina of transgenic mice attenuated ischemia-induced retinal neovascularization, demonstrating its antiangiogenic activities. Furthermore, overexpression of kallistatin ameliorated diabetes-induced retinal leukostasis and vascular leakage. With regard to a mechanism of action, our results demonstrated that kallistatin inhibits the ischemia or diabetes-induced Wnt/β-catenin signaling pathway activation, which has been shown to play a key pathogenic role in DR (14). Further, our results showed that kallistatin inhibits Wnt signaling via antagonizing LRP6. These findings identified kallistatin as a novel, endogenous inhibitor of Wnt signaling and suggest that the decreased retinal levels of kallistatin in diabetes may be responsible, at least in part, for Wnt pathway activation, neovascularization, and neuroinflammation in DR.

Kallistatin was originally identified as an inhibitor of tissue kallikrein (5). Kallistatin was later found to inhibit ischemia-induced limb angiogenesis, and this antiangiogenic activity is independent of its interactions with the tissue kallikrein-kinin system (27). In previous studies, we have reported that kallistatin levels are decreased in the vitreous of patients with DR (8). Accumulating evidence showed that the disturbed balance between proangiogenic factors and antiangiogenic factors in the retina is responsible for pathological retinal neovascularization in DR (28–30). Here, we hypothesized that the decreased levels of kallistatin in DR may disturb the balance between proangiogenic factors and antiangiogenic factors, contributing to retinal neovascularization in DR. To test the hypothesis, we generated transgenic mice overexpressing kallistatin in multiple tissues including the retina. This overexpression strategy resulted in no overt behavioral or developmental abnormalities and no detectable differences in retinal vascular density or distribution between WT and kallistatin-TG mice under normal conditions (Supplementary Fig. 9), suggesting that overexpression of kallistatin in the retina did not affect retinal structure and function (as measured by ERG) under normal conditions. This feature is similar to the results of PEDF transgenic and PEDF knockout mice, which lack overt retinal phenotypes under normal conditions (31).

OIR is a commonly used model of ischemia-induced retinal neovascularization (16,32). Previous studies showed that increased proangiogenic factors and decreased antiangiogenic factors play a key role in ischemia-induced retinal neovascularization in the OIR model (28). The current study demonstrates that endogenous overexpression of kallistatin in transgenic mice ameliorated retinal neovascularization in OIR. Consistently, high levels of kallistatin also attenuated the overexpression of VEGF in the OIR retina. These findings provide the evidence that endogenously expressed kallistatin confers its antiangiogenic activity in the retina, likely through restoring the balance between proangiogenic factors and antiangiogenic factors.

In the OIR model, there are two phases of blood vessel alterations: hyperoxia-induced vessel obliteration in P7–P12 and later ischemia-induced neovascularization in P12–P17 (16,33). The hyperoxia-induced vessel obliteration results in enlarged nonperfusion area in the central retina, a pathological feature characteristic of the OIR model (16,33). Kallistatin displayed dual effects in the OIR model, as it reduced nonperfusion area in the central retina, while inhibiting neovascularization in the peripheral retina. The dual effects have also been reported in other endogenous antiangiogenic factors (31,34–36). Although the mechanism responsible for dual effects of these antiangiogenic factors in the OIR retina is unclear, previous studies suggest that these antiangiogenic factors may reduce hyperoxia-induced vessel obliteration in OIR. Based on previous reports that oxidative stress and vascular inflammation contribute to the vessel obliteration in the OIR model (34,37), we propose that the effect of kallistatin in reducing nonperfusion area may be ascribed to its antioxidant activity (38).

DR, a common microvascular complication of diabetes, is a chronic neuroinflammatory disorder, as shown by overexpression of proinflammatory factors, leukocyte adherence, and infiltration (39). Leukocyte adherence has been shown to impair the endothelium, leading to the blood-retina barrier breakdown and vascular leakage (40). Here, we showed significantly increased leukostasis and vascular leakage in the retina of Akita mice, a type 1 diabetes model, consistent with previous reports (41). When diabetes was induced in kallistatin-TG mice, high levels of kallistatin in the retina attenuated leukostasis and reduced retinal vascular leakage in the Akita model. A recent study found that the major leukocyte subset responsible for diabetic leukostasis in STZ-induced diabetic mice is the CD11b$^+$ leukocytes (presumed to be monocytes) but not Gr-1$^+$ leukocytes or CD3$^+$ T-cells (42). We investigated whether the CD11b$^+$ monocyte was the major cell type involved in leukostasis in the Akita diabetic retina using flow cytometry. Our results confirmed that Akita mice have a significant increase in CD11b$^+$ leukocytes, but no detectable change was observed in Gr-1$^+$ leukocytes, CD19$^+$ B lymphocytes, or CD3$^+$ T lymphocytes. Most importantly, we found that Akita×kallistatin-TG mice had a significant reduction in the CD11b$^+$ leukocytes in the retina, suggesting that the major cell type reduced in the leukostasis assay is the CD11b$^+$ leukocytes. It is thought that CD11b might be an important binding protein of ICAM-1 (42–44), and downregulation of endothelial ICAM-1 levels by kallistatin might result in the reduction of adherent CD11b$^+$ leukocytes in the diabetic Akita×kallistatin-TG retina. Taken together, the downregulation of VEGF and ICAM-1 expression by kallistatin indicates a previously undocumented antineuroinflammatory activity of this SERPIN member.

The canonical Wnt pathway is known to mediate multiple processes including inflammation, angiogenesis, and fibrosis via activation of transcription of multiple inflammatory, angiogenic, and fibrogenic factors (45). Our previous study demonstrated upregulated levels of phosphorylated LRP6 and β-catenin accumulation in the retina of patients with DR and in OIR and diabetic models (14). To further confirm diabetes-induced Wnt signaling activation in the retina, we first induced diabetes in Wnt reporter mice, BAT-gal mice, commonly used reporter mice for Wnt signaling activation (46). Consistent with increased phosphorylation of LRP6 and β-catenin accumulation demonstrated previously (14), BAT-gal mice with diabetes showed more intense X-gal staining in the retina compared with nondiabetic BAT-gal mice, providing a direct evidence of diabetes-induced Wnt signaling in the retina. To investigate whether the antiangiogenic and antineuroinflammatory activities of kallistatin are through interactions with the Wnt pathway in vivo, we crossed the kallistatin-TG mice with the BAT-gal reporter mice. After induction of diabetes, kallistatin-TG mice showed substantially reduced BAT-gal reporter signal compared with diabetic BAT-gal mice in WT background, suggesting suppression of diabetes-induced Wnt signaling by kallistatin. This finding suggests that endogenous expression of kallistatin can inhibit Wnt/β-catenin activation in the retina during DR. The Wnt pathway has been shown to regulate inflammation, angiogenesis, and fibrosis through upregulation of β-catenin target genes such TNF-α, ICAM-1, VEGF, and CTGF and, thus, is believed to play a key role in DR (19,47,48). In both OIR and Akita models, kallistatin transgene overexpression resulted in significantly lower levels of LRP6 and non-pi-β-catenin compared with WT mice without the kallistatin transgene, suggesting that overexpression of kallistatin suppressed Wnt signaling induced by ischemia and by diabetes.

To establish the direct inhibitory effect of kallistatin on Wnt signaling, we evaluated the inhibitory effect of kallistatin on Wnt signaling in cultured cells. Our results showed that either transfection of the kallistatin expression plasmid or treatment with purified kallistatin protein inhibited phosphorylation of LRP6, transcriptional activity of β-catenin, and overexpression of Wnt target genes induced by high-glucose medium and Wnt3a, a canonical Wnt ligand, further confirming the direct inhibition on Wnt signaling. LiCl is commonly used to activate canonical Wnt signaling intracellularly, as it inhibits GSK-3β and subsequently stabilizes β-catenin (49). In the current study, we showed that kallistatin blocks Wnt pathway activation induced by Wnt ligands and by overexpression of LRP6, but not that induced by LiCl, suggesting that kallistatin inhibits Wnt signaling possibly at the Wnt receptor level. This assumption is supported by the specific binding of kallistatin to LRP6, as coimmunoprecipitation assay confirms the physical association of kallistatin with LRP6. Moreover, kallistatin displays a concentration-dependent and saturable binding to the extracellular domain of LRP6 with K_d = 4.5 nmol/L, which is within the range of the physiological concentrations of kallistatin. Further, we showed that Wnt3a dose-dependently competed with kallistatin for binding to LRP6N (Supplementary Fig. 10). Taken together, these findings suggest that kallistatin functions as an endogenous antagonist of LRP6 and a modulator of the Wnt pathway. This mechanism is similar to that of PEDF (48).

In summary, we have identified human kallistatin as a potent inhibitor of angiogenesis and neuroinflammation and an endogenous antagonist of LRP6. Blockade of Wnt signaling by antagonizing LRP6 may represent a unifying mechanism for the antiangiogenic and antineuroinflammatory activities of kallistatin. Decreased levels of kallistatin in the diabetic retina may contribute to the activation of Wnt signaling, leading to retinal neuroinflammation and neovascularization in DR.

REFERENCES

1. Ferrara N, Kerbel RS. Angiogenesis as a therapeutic target. Nature 2005; 438:967–974
2. Dawson DW, Volpert OV, Gillis P, et al. Pigment epithelium-derived factor: a potent inhibitor of angiogenesis. Science 1999;285:245–248
3. Huang H, Campbell SC, Nelius T, et al. Alpha1-antitrypsin inhibits angiogenesis and tumor growth. Int J Cancer 2004;112:1042–1048
4. Miao RQ, Agata J, Chao L, Chao J. Kallistatin is a new inhibitor of angiogenesis and tumor growth. Blood 2002;100:3245–3252
5. Chao J, Chai KX, Chen LM, et al. Tissue kallikrein-binding protein is a serpin. I. Purification, characterization, and distribution in normotensive and spontaneously hypertensive rats. J Biol Chem 1990;265:16394–16401
6. Wolf WC, Harley RA, Sluce D, Chao L, Chao J. Localization and expression of tissue kallikrein and kallistatin in human blood vessels. J Histochem Cytochem 1999;47:221–228
7. Chao J, Yin H, Yao YY, Shen B, Smith RS Jr, Chao L. Novel role of kallistatin in protection against myocardial ischemia-reperfusion injury by preventing apoptosis and inflammation. Hum Gene Ther 2006;17:1201–1213
8. Ma JX, King LP, Yang Z, Crouch RK, Chao L, Chao J. Kallistatin in human ocular tissues: reduced levels in vitreous fluids from patients with diabetic retinopathy. Curr Eye Res 1996;15:1117–1123
9. Jenkins AJ, McBride JD, Januszewski AS, et al. Increased serum kallistatin levels in type 1 diabetes patients with vascular complications. J Angiogenes Res 2010;2:19
10. Reis M, Liebner S. Wnt signaling in the vasculature. Exp Cell Res 2013;319: 1317–1323
11. Logan CY, Nusse R. The Wnt signaling pathway in development and disease. Annu Rev Cell Dev Biol 2004;20:781–810
12. Gong Y, Slee RB, Fukai N, et al.; Osteoporosis-Pseudoglioma Syndrome Collaborative Group. LDL receptor-related protein 5 (LRP5) affects bone accrual and eye development. Cell 2001;107:513–523
13. Toomes C, Bottomley HM, Jackson RM, et al. Mutations in LRP5 or FZD4 underlie the common familial exudative vitreoretinopathy locus on chromosome 11q. Am J Hum Genet 2004;74:721–730
14. Chen Y, Hu Y, Zhou T, et al. Activation of the Wnt pathway plays a pathogenic role in diabetic retinopathy in humans and animal models. Am J Pathol 2009;175:2676–2685
15. Zhang D, Kaufman PL, Gao G, Saunders RA, Ma JX. Intravitreal injection of plasminogen kringle 5, an endogenous angiogenic inhibitor, arrests retinal neovascularization in rats. Diabetologia 2001;44:757–765

16. Smith LE, Wesolowski E, McLellan A, et al. Oxygen-induced retinopathy in the mouse. Invest Ophthalmol Vis Sci 1994;35:101–111

17. Zhang SX, Ma JX, Sima J, et al. Genetic difference in susceptibility to the blood-retina barrier breakdown in diabetes and oxygen-induced retinopathy. Am J Pathol 2005;166:313–321

18. Chen CH, Dixon RA, Ke LY, Willerson JT. Vascular progenitor cells in diabetes mellitus: roles of Wnt signaling and negatively charged low-density lipoprotein. Circ Res 2009;104:1038–1040

19. Zhang B, Abreu JG, Zhou K, et al. Blocking the Wnt pathway, a unifying mechanism for an angiogenic inhibitor in the serine proteinase inhibitor family. Proc Natl Acad Sci USA 2010;107:6900–6905

20. Topol L, Chen W, Song H, Day TF, Yang Y. Sox9 inhibits Wnt signaling by promoting beta-catenin phosphorylation in the nucleus. J Biol Chem 2009; 284:3323–3333

21. Pe'er J, Folberg R, Itin A, Gnessin H, Hemo I, Keshet E. Upregulated expression of vascular endothelial growth factor in proliferative diabetic retinopathy. Br J Ophthalmol 1996;80:241–245

22. Pierce EA, Avery RL, Foley ED, Aiello LP, Smith LE. Vascular endothelial growth factor/vascular permeability factor expression in a mouse model of retinal neovascularization. Proc Natl Acad Sci USA 1995;92:905–909

23. Miller JW, Adamis AP, Shima DT, et al. Vascular endothelial growth factor/vascular permeability factor is temporally and spatially correlated with ocular angiogenesis in a primate model. Am J Pathol 1994;145:574–584

24. Bai Y, Ma JX, Guo J, et al. Müller cell-derived VEGF is a significant contributor to retinal neovascularization. J Pathol 2009;219:446–454

25. Marumo T, Schini-Kerth VB, Busse R. Vascular endothelial growth factor activates nuclear factor-kappaB and induces monocyte chemoattractant protein-1 in bovine retinal endothelial cells. Diabetes 1999;48:1131–1137

26. Barker N, Clevers H. Mining the Wnt pathway for cancer therapeutics. Nat Rev Drug Discov 2006;5:997–1014

27. Chao J, Stallone JN, Liang YM, Chen LM, Wang DZ, Chao L. Kallistatin is a potent new vasodilator. J Clin Invest 1997;100:11–17

28. Gao G, Li Y, Zhang D, Gee S, Crosson C, Ma J. Unbalanced expression of VEGF and PEDF in ischemia-induced retinal neovascularization. FEBS Lett 2001;489:270–276

29. Tombran-Tink J, Barnstable CJ. Therapeutic prospects for PEDF: more than a promising angiogenesis inhibitor. Trends Mol Med 2003;9:244–250

30. Spranger J, Osterhoff M, Reimann M, et al. Loss of the antiangiogenic pigment epithelium-derived factor in patients with angiogenic eye disease. Diabetes 2001;50:2641–2645

31. Huang Q, Wang S, Sorenson CM, Sheibani N. PEDF-deficient mice exhibit an enhanced rate of retinal vascular expansion and are more sensitive to hyperoxia-mediated vessel obliteration. Exp Eye Res 2008; 87:226–241

32. Smith LE. Pathogenesis of retinopathy of prematurity. Acta Paediatr Suppl 2002;91:26–28

33. Connor KM, Krah NM, Dennison RJ, et al. Quantification of oxygen-induced retinopathy in the mouse: a model of vessel loss, vessel regrowth and pathological angiogenesis. Nat Protoc 2009;4:1565–1573

34. Gardiner TA, Gibson DS, de Gooyer TE, de la Cruz VF, McDonald DM, Stitt AW. Inhibition of tumor necrosis factor-alpha improves physiological angiogenesis and reduces pathological neovascularization in ischemic retinopathy. Am J Pathol 2005;166:637–644

35. Banin E, Dorrell MI, Aguilar E, et al. T2-TrpRS inhibits preretinal neovascularization and enhances physiological vascular regrowth in OIR as assessed by a new method of quantification. Invest Ophthalmol Vis Sci 2006;47:2125–2134

36. Bai YJ, Huang LZ, Zhou AY, Zhao M, Yu WZ, Li XX. Antiangiogenesis effects of endostatin in retinal neovascularization. J Ocul Pharmacol Ther 2013;29:619–626

37. Saito Y, Geisen P, Uppal A, Hartnett ME. Inhibition of NAD(P)H oxidase reduces apoptosis and avascular retina in an animal model of retinopathy of prematurity. Mol Vis 2007;13:840–853

38. Shen B, Gao L, Hsu YT, et al. Kallistatin attenuates endothelial apoptosis through inhibition of oxidative stress and activation of Akt-eNOS signaling. Am J Physiol Heart Circ Physiol 2010;299:H1419–H1427

39. Shah CA. Diabetic retinopathy: A comprehensive review. Indian J Med Sci 2008;62:500–519

40. Xu H, Forrester JV, Liversidge J, Crane IJ. Leukocyte trafficking in experimental autoimmune uveitis: breakdown of blood-retinal barrier and upregulation of cellular adhesion molecules. Invest Ophthalmol Vis Sci 2003;44:226–234

41. Barber AJ, Antonetti DA, Kern TS, et al. The Ins2Akita mouse as a model of early retinal complications in diabetes. Invest Ophthalmol Vis Sci 2005;46: 2210–2218

42. Serra AM, Waddell J, Manivannan A, Xu H, Cotter M, Forrester JV. CD11b+ bone marrow-derived monocytes are the major leukocyte subset responsible for retinal capillary leukostasis in experimental diabetes in mouse and express high levels of CCR5 in the circulation. Am J Pathol 2012;181:719–727

43. Diamond MS, Springer TA. A subpopulation of Mac-1 (CD11b/CD18) molecules mediates neutrophil adhesion to ICAM-1 and fibrinogen. J Cell Biol 1993;120:545–556

44. Diamond MS, Staunton DE, de Fougerolles AR, et al. ICAM-1 (CD54): a counter-receptor for Mac-1 (CD11b/CD18). J Cell Biol 1990;111:3129–3139

45. Klaus A, Birchmeier W. Wnt signalling and its impact on development and cancer. Nat Rev Cancer 2008;8:387–398

46. Maretto S, Cordenonsi M, Dupont S, et al. Mapping Wnt/beta-catenin signaling during mouse development and in colorectal tumors. Proc Natl Acad Sci USA 2003;100:3299–3304

47. Lee K, Hu Y, Ding L, et al. Therapeutic potential of a monoclonal antibody blocking the Wnt pathway in diabetic retinopathy. Diabetes 2012;61:2948–2957

48. Park K, Lee K, Zhang B, et al. Identification of a novel inhibitor of the canonical Wnt pathway. Mol Cell Biol 2011;31:3038–3051

49. Cha B, Kim W, Kim YK, et al. Methylation by protein arginine methyltransferase 1 increases stability of Axin, a negative regulator of Wnt signaling. Oncogene 2011;30:2379–2389